

## OPTICAL PROPERTIES OF THE QUASI-PERIODIC ONE-DIMENSIONAL GENERALIZED MULTILAYER FIBONACCI STRUCTURES

M. Aissaoui, J. Zaghdoudi, M. Kanzari, and B. Rezig

Laboratoire de Photovoltaïque et Matériaux Semiconducteurs  
Département Génie Industriel  
Ecole Nationale d'Ingénieurs de Tunis  
BP 37, Belvédère, 1002 Tunis, Tunisia

**Abstract**—Optical properties of generalized dielectric Fibonacci multilayer generated by the rule  $S_{l+1} = S_l^n S_{l-1}^m$  with a pair of positive integers  $m$  and  $n$  were studied. The initial generations  $S_1$  and  $S_2$  are taken as  $S_1 = H$  and  $S_2 = L$  where  $H$  and  $L$  are two elementary layers with refractive indices  $n_L = 1.45$  and  $n_H = 2.3$ , respectively. In the following numerical investigation, we chose  $\text{SiO}_2$  ( $L$ ) and  $\text{TiO}_2$  ( $H$ ) as two elementary layers. We use the so-called “antitrace” map to determine the transmission spectra of the structures. Based on the representation of the transmittance spectra in the visible range an analysis depending on the pair  $(n, m)$  is presented. We show that the whole structure  $S_l^n S_{l-1}^m$  has an interesting application for well selection pairs  $(m, n)$  values.

### 1. INTRODUCTION

Photonic crystals (PCs) have attracted much attention because they are interesting objects of study in physics and because of their potential applications to various optical devices such as micro optical circuits and single mode light-emitting diodes [1–4]. It is known that three-dimensional (3D) photonic crystals can achieve a complete photonic bandgap (PBG). Unfortunately, there are still two formidable difficulties in applying 3D photonic crystals as devices: One is making 3D periodic dielectric structures with a feature size comparable to the wavelength of visible light; the other is achieving dielectric contrasts to obtain a forbidden gap that overlaps in all directions within the Brillouin zone. Compared with the 3D case, one-dimensional

(1D) photonic crystals, i.e., dielectric multilayers, are much easier to fabricate.

In recent years, there has been much interest in the physics and applications of one-dimensional spatially periodic, quasiperiodic and random photonic bandgap (PBG) structures [5, 6]. Quasi-periodic systems can be considered as suitable models to describe the transition from the perfect periodic structure [7] to the random structure [8, 9]. If made from dielectric material, the resulting structure has interesting optical properties. The most important and well-known quasi-periodic structure is the Fibonacci sequence (FS) [10, 11]. Quasicrystals are non-periodic structures that are constructed following a simple deterministic generation rule [12]. If made from dielectric material, the resulting structure has interesting optical properties. Quasicrystals of the Fibonacci type, for instance, exhibit an energy spectrum that consists of a self-similar Cantor set with zero Lebesgue measure [13]. The transmission spectrum of a Fibonacci system also contains forbidden frequency regions called pseudo-bandgaps similar to the bandgaps of a photonic crystal [14, 15]. In the frequency regime outside the Fibonacci band gaps, the light waves are critically localized.

This study deals with the optical properties of the quasi-periodic one-dimensional multilayer. The quasi-crystal is constructed by applying an iterative recipe, called generating rule, to a set of “building blocks” (layers with defined thickness and refractive index). The Fibonacci structure is the most studied quasi-crystal because of its simple generating recipe. In this work we use the generated Fibonacci sequence constructed by the rule  $F_{l+1} = F_l^n F_{l-1}^m$  with a pair of positive integer's  $m$  and  $n$ , for normal incidence in the visible spectral range  $[0.4, 0.8] \mu\text{m}$ .

## 2. MODEL AND FORMALISM

There are many kinds of generalized Fibonacci sequences FSs  $(n, m)$ . Here, we study a system of a Fibonacci multilayer of two materials  $H$  and  $L$  as follows (Fig. 1):

$$\begin{aligned} F_1 &= H, F_2 = L \\ F_{l+1} &= F_l^n F_{l-1}^m, \text{ for } l \geq 3, \end{aligned}$$

with arbitrary integers  $n$  and  $m$ . It was assumed that:

- Incident wave has  $S$  polarization
- Optical thicknesses of  $H$  and  $L$  layers are equal
- Neither reflection or refraction occurs on the interfaces between the system and external media

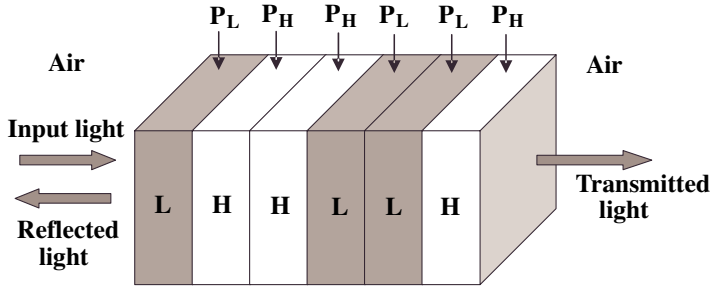


**Figure 1.** The model of the study configuration Fibonacci sequence.

The corresponding transfer matrices  $S_l$  are written as:

$$\begin{aligned}
 S_1 &= P_{(air/L)}P_LP_{(L/air)} \\
 S_2 &= P_{(air/H)}P_HP_{(H/air)} \\
 \forall l \geq 3 \quad S_{l+1} &= S_l^m S_{l-1}^m
 \end{aligned} \tag{1}$$

where  $P_{(air/L)}$  ( $P_{(L/air)}$ ) stands for the propagation matrix from the air ( $L$ ) to  $L$  (the air) and  $P_L$  is the propagation matrix through single layer  $L$ .

In the same way,  $P_{(air/H)}$  ( $P_{(H/air)}$ ) stands for the propagation matrix from the air ( $H$ ) to  $H$  (the air) and  $P_H$  is the propagation matrix through the single layer  $H$ .

These transfer matrices are given by:

$$\begin{aligned}
 P_{(air/L)} = P_{(L/air)}^{-1} &= \begin{pmatrix} 1 & 0 \\ 0 & 1/n_L \end{pmatrix} & P_L &= \begin{pmatrix} \cos(\delta_L) & -\sin(\delta_L) \\ \sin(\delta_L) & \cos(\delta_L) \end{pmatrix} \\
 P_{(air/H)} = P_{(H/air)}^{-1} &= \begin{pmatrix} 1 & 0 \\ 0 & 1/n_H \end{pmatrix} & P_H &= \begin{pmatrix} \cos(\delta_H) & -\sin(\delta_H) \\ \sin(\delta_H) & \cos(\delta_H) \end{pmatrix}
 \end{aligned}$$

where  $\delta_{H(L)} = kn_{H(L)}d_{H(L)}$ ,  $n_{H(L)}$  is the refractive index of media  $H(L)$ ,  $d_{H(L)}$  is the layer thicknesses, and  $k$  is the wave number in vacuum. Generally, we choose appropriate layer thicknesses  $d_H$  and  $d_L$  to make  $n_H d_H = n_L d_L$ . Then we have  $\delta_L = \delta_H = \delta$ .

The transmission coefficient is given by [16]:

$$T_l = \frac{4}{|S_i|^2 + 2}$$

where  $|S_i|^2$  is the sum of squares of the four elements of the matrix  $S_l$ , since the transfer matrix is unimodular, the transmission coefficient

can be written as:

$$T_l = \frac{4}{x_l^2 + y_l^2}$$

where  $x_l$  and  $y_l$  denote respectively the trace and antitrace of the transfer matrix  $S_l$ .

Given a matrix  $A = \begin{pmatrix} A_{11} & A_{12} \\ A_{21} & A_{22} \end{pmatrix}$ , the antitrace of  $A$  is defined as  $y_A = A_{21} - A_{12}$ .

The  $n^{\text{th}}$  power of a unimodular  $2 \times 2$  matrix  $A$  is given by:

$$A^n = U_n(x_A)A - U_{n-1}(x_A)I \quad (2)$$

where  $I$  is the unit matrix and

$$U_n(x_A) = \frac{\lambda_+^n - \lambda_-^n}{\lambda_+ - \lambda_-}, \quad \lambda_{\pm} = \frac{x_A \pm \sqrt{x_A^2 - 4}}{2}$$

where  $x_A$  and  $\lambda_{\pm}$  denote the trace and the eigen values of  $A$ , respectively.

Using Eqs. (1) and (2), we can write the recursion relation of the transfer matrix as:

$$S_{l+1} = (U_n(x_l)S_l - U_{n-1}(x_l)I) \cdot (U_m(x_{l-1})S_{l-1} - U_{m-1}(x_{l-1})I) \quad (3)$$

So, to study the antitrace maps, we need the following identity for two unimodular transfer matrices  $H$  and  $L$ :

$$Y_{(HL)} = X_L \cdot Y_H + X_H \cdot Y_L - Y_{(LH)} \quad (4)$$

The recursion relation of the trace and the antitrace map, can be written as (for  $l \in \mathbb{N}$ ):

$$\begin{aligned} X_{l+1} &= U_n(X_l) \cdot U_m(X_{l-1}) \cdot V_l \\ &\quad - U_{n-1}(X_l) \cdot U_{m+1}(X_{l-1}) - U_{n+1}(X_l) \cdot U_{m-1}(X_{l-1}) \\ V_{l+1} &= U_{n+1}(X_l) \cdot U_m(X_{l-1}) \cdot V_l \\ &\quad - U_n(X_l) \cdot U_{m+1}(X_{l-1}) - U_{n+2}(X_l) \cdot U_{m-1}(X_{l-1}) \\ Y_{l+1} &= U_n(X_l) \cdot U_m(X_{l-1}) \cdot W_l \\ &\quad - U_{n-1}(X_l) \cdot U_m(X_{l-1}) \cdot Y_{l-1} - U_n(X_l) \cdot U_{m-1}(X_{l-1}) \cdot Y_l \\ W_{l+1} &= X_{l+1} \cdot Y_l + U_{n-1}(X_l) \cdot U_m(X_{l-1}) \cdot W_l \\ &\quad - U_{n-2}(X_l) \cdot U_m(X_{l-1}) \cdot Y_{l-1} - U_{n-1}(X_l) \cdot U_{m-1}(X_{l-1}) \cdot Y_l \end{aligned}$$

where  $V_l = \text{trace}(S_l S_{l-1})$  and  $W_l = \text{antitrace}(S_l S_{l-1})$ .

Consequently, the trace and antitrace map are completely determined by these relations. The forms of trace and antitrace maps are easy to be obtained and are convenient for application. If we know the initial conditions, the transmission coefficients can be determined from the trace and antitrace map.

### 3. RESULTS AND DISCUSSION

The factors influencing the system response are the choice of first two iterations  $A_1$  and  $A_2$ , the choice of the parameter  $m$ , the choice of the parameter  $n$  and the choice of the iteration  $l$ . In the following numerical investigation, we chose  $\text{SiO}_2$  ( $L$ ) and  $\text{TiO}_2$  ( $H$ ) as two elementary layers, with refractive indices  $n_L = 1.45$  and  $n_H = 2.3$ , respectively.

#### 3.1. The Number and Nature of the Layers

For a quasiperiodic multilayer ordered according to the generalized Fibonacci, in the  $l^{\text{th}}$  iteration, the total number of layers ( $F_l$ ), the number of high indices' layers ( $H_l$ ) and the number of low indices' layers ( $L_l$ ) are determined by (for  $l \in \mathbb{N}$ ):

$$F_l = -\frac{(n-2) - \sqrt{n^2 + 4m}}{2 \cdot \sqrt{n^2 + 4m}} \left( \frac{n + \sqrt{n^2 + 4m}}{2} \right)^{l-1} + \frac{(n-2) + \sqrt{n^2 + 4m}}{2 \cdot \sqrt{n^2 + 4m}} \left( \frac{n - \sqrt{n^2 + 4m}}{2} \right)^{l-1} \quad (5)$$

$$H_l = \frac{1}{\sqrt{n^2 + 4m}} \left( \frac{n + \sqrt{n^2 + 4m}}{2} \right)^{l-1} - \frac{1}{\sqrt{n^2 + 4m}} \left( \frac{n - \sqrt{n^2 + 4m}}{2} \right)^{l-1} \quad (6)$$

$$L_l = \frac{m}{\sqrt{n^2 + 4m}} \left( \frac{n + \sqrt{n^2 + 4m}}{2} \right)^{l-2} - \frac{m}{\sqrt{n^2 + 4m}} \left( \frac{n - \sqrt{n^2 + 4m}}{2} \right)^{l-2} \quad (7)$$

In the iteration  $l \geq 3$ , the system contains  $F_l (= n \cdot F_{l-1} + m \cdot F_{l-2})$  dielectric layer. We consider  $j_l \in \langle 1, F_l \rangle$ , the refraction indices in the  $j^{\text{th}}$  layer:

- If  $j_l \in \langle 1, n \cdot F_{l-1} \rangle$  then it exists  $j_{l-1} \in \langle 1, F_{l-1} \rangle$  such as  $j_l \equiv j_{l-1}[F_{l-1}]$ , then  $n[j_l] = n[j_{l-1}]$

- If  $j \in \langle n \cdot F_{l-1} + 1, F_l \rangle$ , it exists  $j_{l-2} \in \langle 1, F_{l-2} \rangle$  such as  $(j - n \cdot F_{l-1}) \equiv j_{l-2}[F_{l-2}]$ , then  $n[j] = n[j_{l-2}]$   
 If  $n[j_l] = n[j_{l-1}]$ , the same calculation is redone with  $j_{l-1}$  at the iteration  $(l - 1)$   
 If  $n[j_l] = n[j_{l-2}]$ , the same calculation is redone with  $j_{l-1}$  at the iteration  $(l - 2)$

### 3.2. Effect of the Iteration

Independently of the obtained spectra nature which will be discussed later, we noticed that when the number of iteration ( $l$ ) increases, the spectra's bands become narrower and more and more cumbersome at all the couple  $(n, m)$ . For the Sections 3.3 and 3.4 we choose the 6<sup>th</sup> generation.

### 3.3. The Effect of the $m$ Variation with $n$ Fixed to 1

The obtained transmission spectra show that the optical properties of the system depend on the parity of  $m$ .

#### 3.3.1. Case $m$ Even

The various spectra (Fig. 2) present bands of oscillations, one of which is centred always in  $\lambda_0 = 0.5 \mu\text{m}$ . These bands narrow and the number of oscillations increase as  $m$  increases. Besides, the number of the peaks around  $\lambda_0$  is governed approximately by a simple linear function according to  $m$  by (Fig. 3):

$$N = 1.27273 + 1.34545 \cdot m$$

This allows us to predict the number of peaks and without making calculation which becomes complex for the great  $m$  values.

On the other hand, the transmission bandwidth  $\Delta\lambda$  around  $\lambda_0 = 0.5 \mu\text{m}$  is decreasing as an exponential function with  $m$  increasing and then it tends to be constant while  $m$  takes great values (Fig. 4). By increasing the  $m$  number, more bands, which present oscillations and gradually emerge (shown in Figs. 2(b)–(d)).

#### 3.3.2. Case $m$ Odd

The various spectra (Fig. 5) present around  $\lambda_0 = 0.5 \mu\text{m}$  a spectral band with weak transmission value. It is clear from the figure that the transmission band tends towards zero as  $m$  increases.

On the other hand, the reflection bandwidth  $\Delta\lambda$  around  $\lambda_0 = 0.5 \mu\text{m}$  is decreasing as an exponential function with  $m$  increasing and

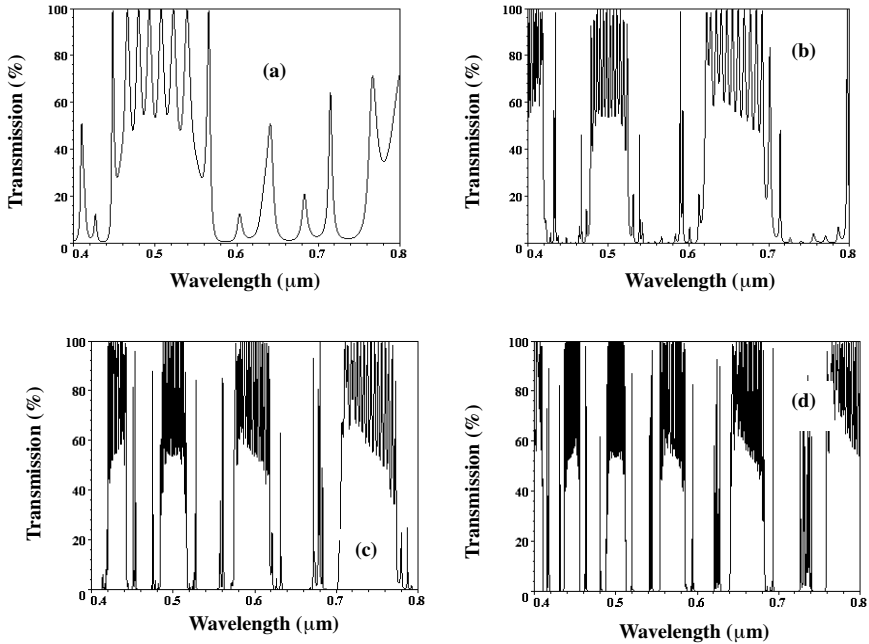


**Figure 2.** Transmission properties of a quarter-wave stack of the FS  $(1,m)$  system for the 6<sup>th</sup> generation at normal incidence as a function of wavelength for (a)  $m = 4$ ; (b)  $m = 6$ ; (c)  $m = 12$ ; (d)  $m = 16$ .

then it tends to be constant while  $m$  takes great values (Fig. 6). Besides, more bands which present oscillations gradually emerge (shown in Figs. 5(b)–(d)), by increasing the  $m$  number.

According to Figs. 2 and 5, there are indeed multiples bands in the generalized dielectric Fibonacci dielectric multilayer, but the band positions depend with the parity of the  $m$  number.

The results mean that under the special conditions given above, the system around  $\lambda_0 = 0.5 \mu\text{m}$  shows a switchlike property with “off” for the odd generation and “on” for the even generation.

### 3.4. The Effect of the $n$ Variation with $m$ Fixed to 1

To study the transmission properties, we classify the FSs  $(n, 1)$  to two families: the even family with  $n = 2m$  and the odd one with  $n = 2m+1$ ,  $m = 0, 1, 2, 3, \dots$

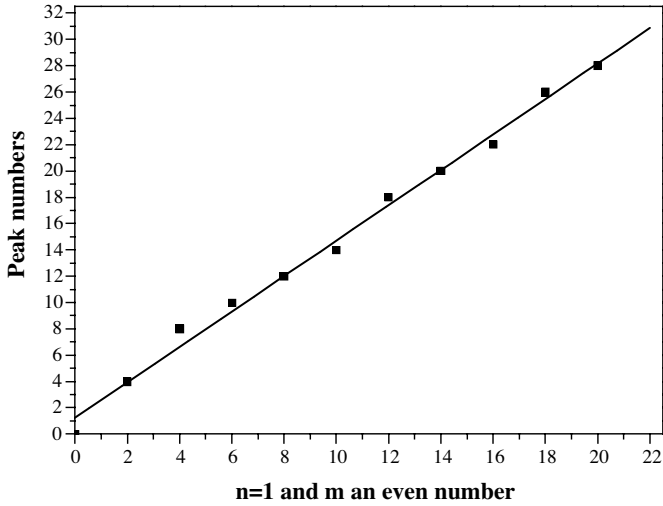


**Figure 3.** Behaviour of the peak numbers around  $\lambda_0 = 0.5 \mu\text{m}$  versus  $m$  odd number for  $n = 1$ .

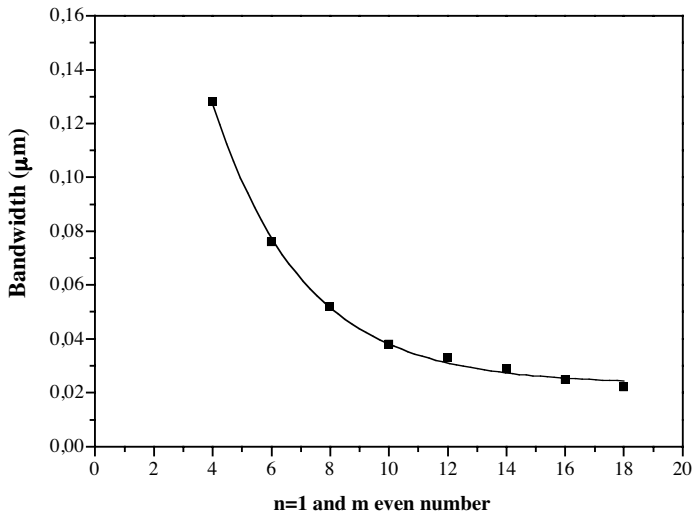


**Figure 4.** Plots of the bandwidth around the reference wavelength  $\lambda_0$  versus  $m$  even number for  $n = 1$ .

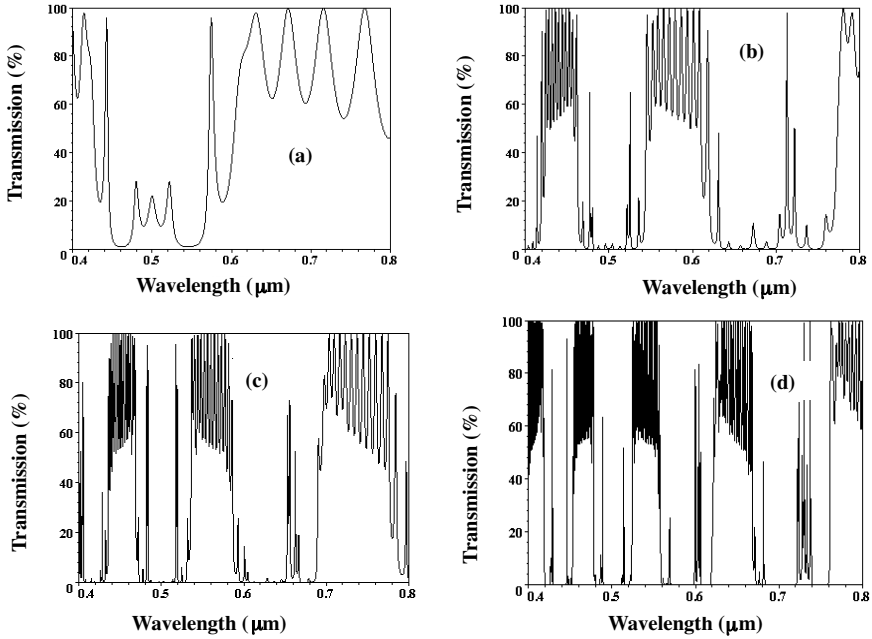


**Figure 5.** Transmission properties of a quarter-wave stack of the FS  $(1, m)$  system for the 6<sup>th</sup> generation at normal incidence as a function of wavelength for (a)  $m = 3$ ; (b)  $m = 7$ ; (c)  $m = 9$ ; (d)  $m = 13$ .

3.4.1. Case  $n$  Even

The system responses (Fig. 7) show a multitude of fixed bands, which increased and contracted by  $n$  increasing (see Fig. 7(e)). We note that for  $n \geq 4$  we can count around  $\lambda_0$  the number of peaks in the bands at the 6<sup>th</sup> iteration which obeys to the following law:

$$N_6(n) = n^2 \cdot (n - 1)$$

3.4.2. Case  $n$  Odd

The measured transmission spectra are shown in Fig. 8 for different odd numbers. The spectra show a multitude of peaks in particular around  $\lambda_0$ . The number of peaks around  $\lambda_0$  can be determined at the 6<sup>th</sup> iteration according to  $n$  by the following law:

$$N_6(n) = n^2$$

As we can see from the Fig. 8, the peaks bands increase and contracted with  $n$  increasing. It appears from Fig. 8(c) that no peaks are observed

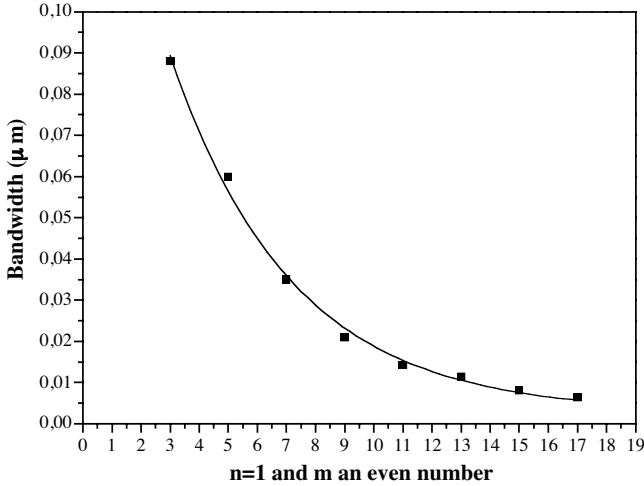


**Figure 6.** Plots of the bandwidth around the reference wavelength  $\lambda_0$  versus  $m$  an even number for  $n = 1$ .

but in reality the peaks are contracted in a weak spectral range and Figs. 8(e) and 8(f) confirm this observation. So, quasiperiodic multilayers ordered according to the generalized Fibonacci for  $m = 1$  and  $n$  odd are polychromatic filters in the field of the visible and for which performances increase when  $n$  increases. These filters present the advantage to have a very close optical windows as  $n$  increases. However the width of the total band around  $\lambda_0$  decreases when  $n$  increase and peaks get closer some of the others.

### 3.4.3. Autosimilarity

It is known that the sequences FS  $(m, n)$  with  $n > 1$  are quasiperiodic and those with  $n > 2$  are always aperiodic [10]. Indeed, the fractal aspect is verified for these systems for  $m = 1$  and  $n$  variable. (Fig. 10). Or according to Lavrinenko and al [11], the determination of the wavelength domain for which the transmission spectra of the system at the iteration  $l$  is similar to that of at the iteration  $(l - 1)$  is not unpredictable. Indeed, they demonstrated that for multilayers' systems with Cantor distribution which are fractal structures, and in a centred domain around  $\lambda_0$ , the transmission spectra of the system at the iteration  $(N - 1)$  with a width domain  $\Delta_{N-1}$  is similar in that of at the itéraion  $N$  on a width domain  $\Delta_N$  which equal to  $\Delta_{N-1}/G$ , with  $G$  is the report of the layers numbers of two consecutive iterations (For example  $G = 3$  for systems with distribution of classic Cantor).

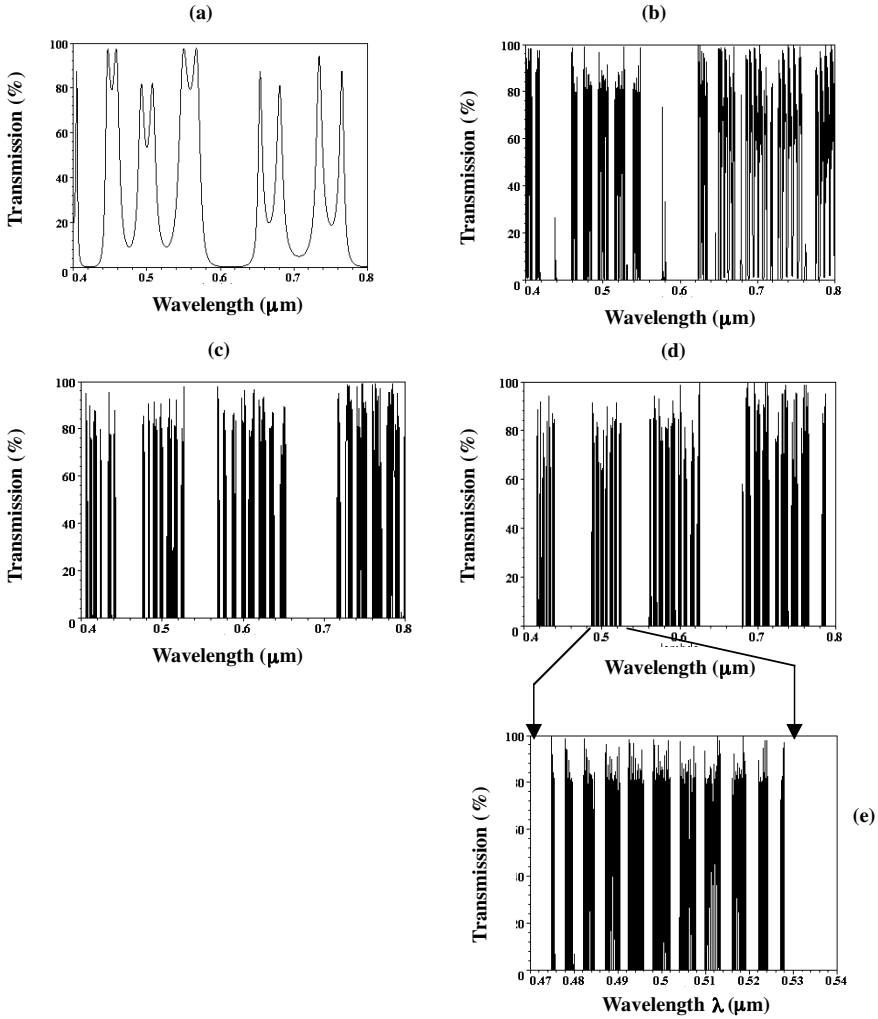


**Figure 7.** Transmission properties of a quarter-wave stack of the FS  $(n, 1)$  system for the 6<sup>th</sup> generation at normal incidence as a function of wavelength for (a)  $n = 2$ ; (b)  $n = 6$ ; (c)  $n = 10$ ; (d)  $n = 12$ ; (e) case  $n = 12$  for the spectral range around the reference wavelength  $\lambda_0$ .

By analogy, we define  $d(n, m)$  as being the limit of the report of the layers number of two consecutive iterations which given by:

$$d(n, m) = \lim_{l \rightarrow +\infty} \frac{F_{l+1}}{F_l} = \frac{n + \sqrt{n^2 + 4m}}{2}$$

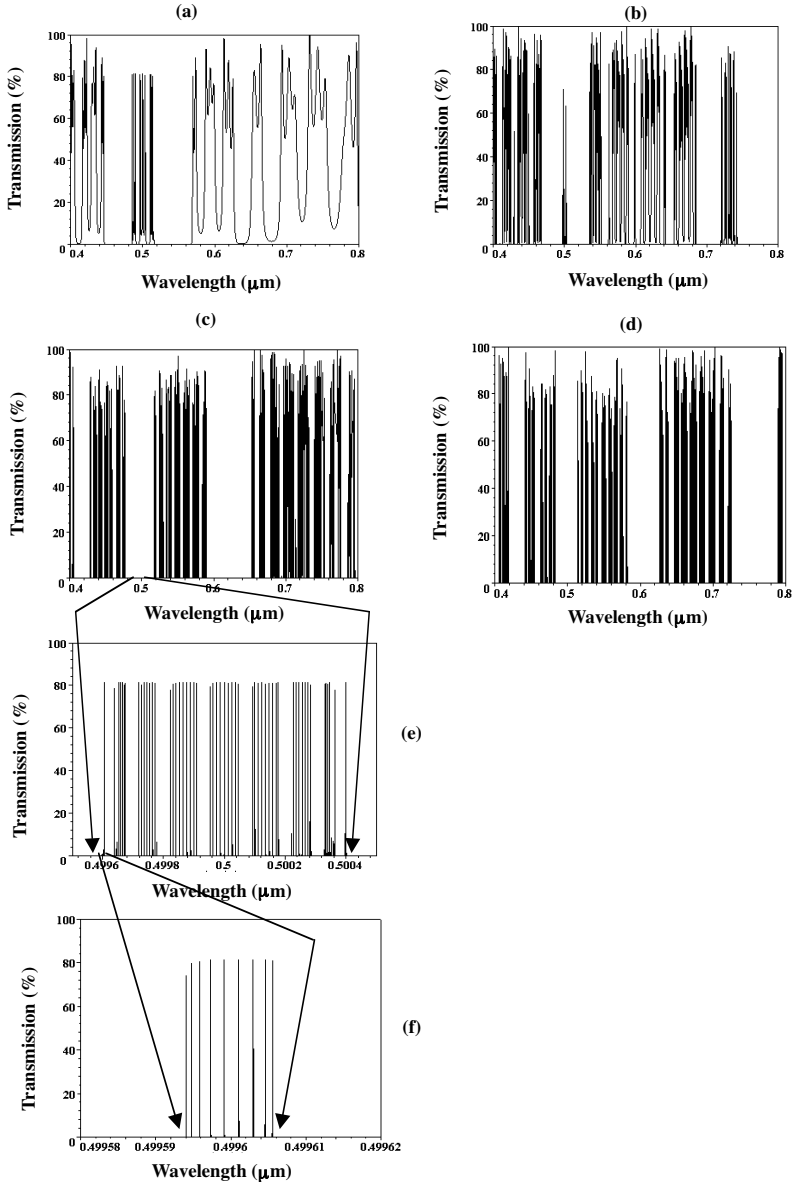


**Figure 8.** Transmission properties of a quarter-wave stack of the FS  $(n, 1)$  system for the  $6^{th}$  generation at normal incidence as a function of wavelength for (a)  $n = 3$ ; (b)  $n = 5$ ; (c)  $n = 9$ ; (d)  $n = 11$ ; (e) case  $n = 9$  for the spectral range around the reference wavelength  $\lambda_0$ ; (f) case  $n = 9$  for the spectral range around the wavelength  $0.4996 \mu\text{m}$ .

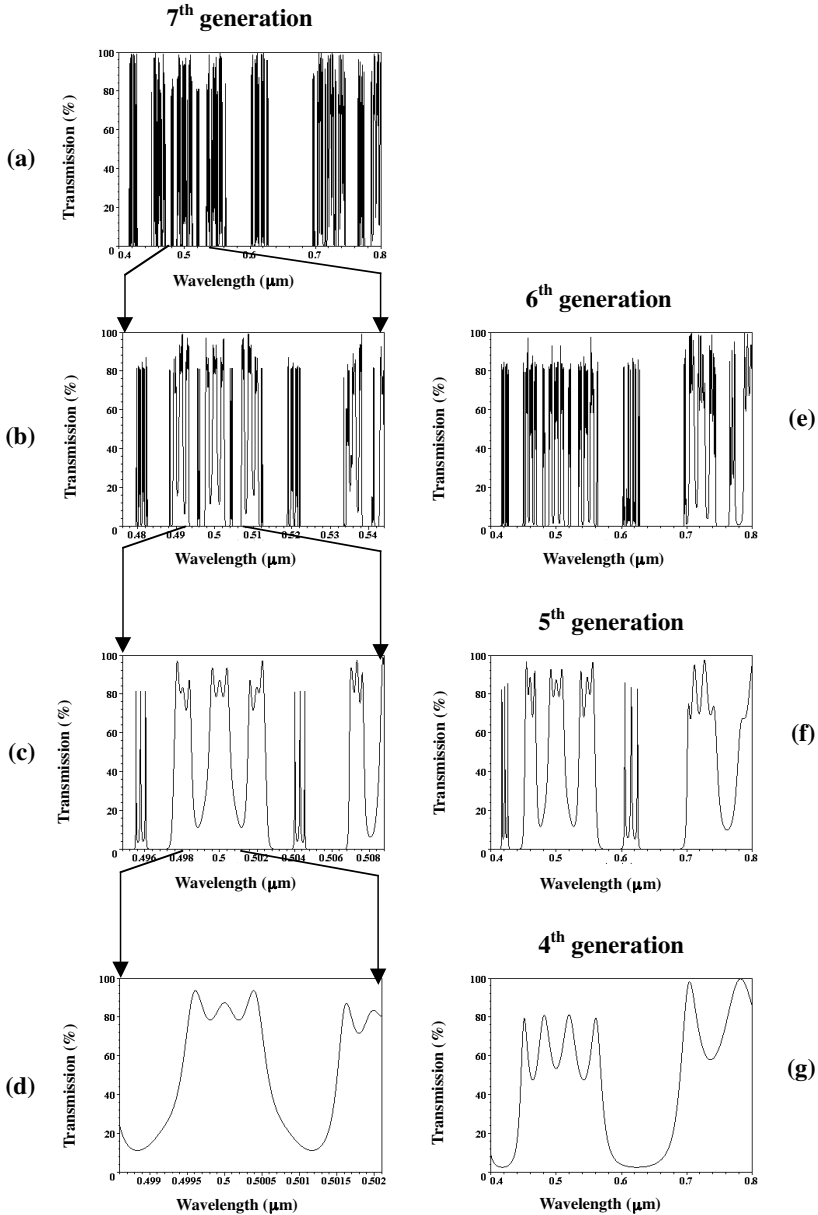


**Figure 9.** Autosimilarity aspect of transmission spectra of the generalized Fibonacci sequence FS (4,1). Scalability can be seen clearly if one compares (a) with (e), and (c) with (f) and (d) with (g).

For example for  $n = 4$  and  $m = 1$  than  $d(4, 1) = 4.23$ .

So, If we scale the part of the spectral range centered at the reference wavelength  $\lambda_0 = 0.5 \mu\text{m}$  in a  $(d, l)$ -structure spectrum by a factor of  $d$ , it will match the spectrum of  $(d, l - 1)$  almost perfectly (see Fig. 9). If the scaling factor is  $d^2$ , we will obtain an  $l$ -2<sup>th</sup> generation spectrum, and so on, up to  $l = 0$ . We have called this property *spectral scalability*, found it to be inherent to all Cantor Fibonacci structures.

This scalability directly results from self-similarity of the structures themselves which obey *the same* scaling relations, i.e., a  $(d, l)$ -structure contains fragments which, scaled by  $d^n$ , match the structures of previous generations. This way, a direct correlation between geometrical and spectral properties of Fibonacci multilayers is established.

#### 4. CONCLUSION

In conclusion, we have investigated for normal incidence of light the transmission properties through the generalized Fibonacci quasiperiodic multilayers FS  $(m, n)$  and found some interesting results. We established direct correlation between geometrical and spectral properties of generalized Fibonacci multilayer structures. Three interesting physical situations described in the sections 3.3 and 3.4 have been considered. The first proposed approach for  $n > 1$  and  $m = 1$  can be applied in design of optical devices or instruments like polychromatic filters. The second and when  $n = 1$  and  $m$  is an odd number the FS  $(m = 2p, 1)$  multilayers displays a switchlike property (on-off-on-off- ... ) which can be applied as an optical switching. Finally, we observe for FS  $(n, 1)$  a scaling of the transmission coefficient with increasing Fibonacci sequences and the value  $n$  at quarter-wavelength optical thicknesses. This behaviour is in good agreement with theory and can be considered as experimental evidence for the localization of the light waves.

#### REFERENCES

1. Soukoulis, C. M., *Photonic Band Gaps and Localization*, Plenum, New York, 1993.
2. Joannopoulos, J., R. Meade, and J. Winn, *Photonic Crystals*, Princeton Press, Princeton, 1995.
3. Soukoulis, C. M., *Photonic Band Gap Materials*, Kluwer Academic Publishers, Dordrecht, 1996.

4. Rarity, J. and C. Weisbuch, *In Microcavities and Photonic Bandgaps, Physics and Applications*, Kluwer Academic Publishers, Dordrecht, 1996.
5. Joannopoulos, J. D., R. D. Meade, and J. N. Winn, *Photonic Crystals: Molding the Flow of Light*, Princeton University Press, Princeton, NJ, 1995.
6. Soukoulis, C. M., *Photonic Crystals and Light Localization in the 21<sup>st</sup> Century*, Kluwer, Dordrecht, 2001.
7. Chigrin, D. N., A. V. Laverinko, D. A. Yarotsky, and S. V. Gaponenko, "All-dielectric one-dimensional periodic structures for total omnidirectional reflection and spontaneous emission control," *J. Light. Technol.*, Vol. 17, 2018, 1999.
8. Zhang, D. Z., Z. L. Li, W. Hu, and B. Y. Cheng, "Broad-band optical reflector — an application of light localization in one-dimension," *Appl. Phys. Lett.*, Vol. 67, 2431, 1995.
9. Han, P. and H. Z. Wang, "Effect of invariant transformation in one-dimensional randomly-perturbed photonic crystal," *Chin. Phys. Lett.*, Vol. 20, 1520, 2003.
10. Merlin, R., K. Bajema, R. Clarke, F. Y. Juang, and P. K. Bhattacharya, "Quasiperiodic GaAs-AlAs heterostructures," *Phys. Rev. Lett.*, Vol. 55, 1768, 1985.
11. Kohmoto, M., B. Sutherland, and K. Iguchi, "Localization of optics: quasiperiodic media," *Phys. Rev. Lett.*, Vol. 58, 2436, 1987.
12. Fujiwara, T. and T. Ogawa, "Chains, flowers, rings and peanuts: graphical geodesic lines and their application to penrose tiling," *Quasicrystals, Springer Series in Solid-State Sciences*, Springer Verlag, Berlin, Vol. 93, 1990.
13. Gumbs, G. and M. K. Ali, "Dynamical maps, cantor spectra, and localization for fibonacci and related quasiperiodic lattices," *Phys. Rev. Lett.*, Vol. 60, 1081, 1988.
14. Nori, F. and J. P. Rodriguez, "Acoustic and electronic properties of one-dimensional quasicrystals," *Phys. Rev. B*, Vol. 34, 2207, 1986.
15. Capaz, R. B., B. Koiller, and S. L. A. de Queiroz, "Gap states and localization properties of 1-D fibonacci quasicrystals," *Phys. Rev. B*, Vol. 42, 6402, 1990.
16. Wang, X., U. Grimm, and M. Schreiber, "Trace and antitrace maps for aperiodic sequences, their extensions and applications," *Phys. Rev. B*, Vol. 62, 14020–14031, 2000.